Asymptotic study of film thinning process on a spinning annular disk

B. S. Dandapat
Physics and Applied Mathematics Unit, Indian Statistical Institute, Calcutta 700035, India

Prabir Daripa[a)]
Department of Mathematics, Texas A&M University, College Station, Texas 77843

P. C. Ray
Physics and Applied Mathematics Unit, Indian Statistical Institute, Calcutta 700035, India

(Received 8 April 2003; accepted 23 June 2003)

We consider an axisymmetric flow of a thin liquid film on a rotating annular disk. The effects of surface tension and gravity terms are included. An asymptotic solution for the free surface of the thin film is found using an expansion for the film thickness in powers of a small parameter characterizing the film thickness in comparison to the inner disk radius, and then applying the method of matched asymptotic expansion. The asymptotic solution is capable of predicting several features of spin-coating processes. For example, we find that the surface tension enhances film thinning at the central region whereas the gravity does not. The results show that the final film thickness does not depend on the initial distribution of the film thickness (be it uniform or nonuniform) and on the initial amount of liquid deposited. We find that most of the liquid initially deposited on the disk flows out of the disk in a very short time at the initial stages of spinning, regardless of the type of initial distribution of the film thickness. The retention of fluid for nonuniform initial distribution is more than that for uniform distribution at the early stages of the spreading of the thin film. [DOI: 10.1063/1.1600826]

I. INTRODUCTION

The production of thin films on solid surfaces has enormous practical applications. Thin liquid films can be produced on smooth solid surfaces either by the action of gravity on stationary vertical/inclined planes or by the action of centrifugal force on rotating disks. The pioneering work of Kapitza[1] on thin viscous fluid layers has been a catalyst for extensive research on the production of thin liquid films under gravity. However, similar studies under centrifugal force, instead of gravity, have received much less attention, in spite of the fact that the centrifugal force can be controlled at any desired level in a proper laboratory setting.

The importance of thin-film production on a rotating disk has gained significant momentum over last two decades in connection with the coating on integrated circuit chips and other substrates in the microelectronics industry. A theoretical study of the associated viscous flow in this field was carried out by Emslie *et al.*[2] more than forty years ago. They considered the axisymmetric flow of a Newtonian fluid on a planar substrate rotating with constant angular velocity and assumed that a steady state would be reached when centrifugal and viscous forces were balanced. A study of this simplified problem allowed the authors to show that the uniformity of the film is not disturbed as the film thins gradually. Subsequent authors have extended this work to include various physical factors including surface tension, air shear, non-Newtonian fluids, nonplanar substrate, evaporation, and adsorption. In connection to this, the article of Larson and Rehg[3] should also be reviewed.

Over the past three decades, various authors have attempted to explain and understand the various relations among different factors involved in spin-coating process. Careful experiments[4,5] have shown that the final film thickness is largely insensitive to the initial amount of fluid deposited on the disk, the rate of removal of the fluid, the rotational acceleration, and even the total spin time. A strong dependence was observed for the initial solute concentration and the final spin speed by Meyerhofer.[4] Sukanek[5] proceeded further to consider the effects of evaporation rate on the spin speed and solute concentration. Jenekhe and Schuldt[6] extended this problem to the case of non-Newtonian fluid and studied the effects of elasticity on this flow. Lawrence[7] extensively reviewed some of the main contributions to the theory, as well as the experimental observations. But all of these analyses were based on the typical hydrodynamical approximation as employed by Emslie *et al.*[2]

Full Navier–Stokes equations were considered by Higgins[8] to study the flow development through a matched asymptotic expansion procedure. Later, Dandapat and Ray[9–11] and Ray and Dandapat[12] extended the problem to analyze the effects of thermocapillarity and magnetic field on the rate of film thinning. They observed that the thermocapillary effect plays a vital role in enhancing the film thinning rate. In these studies, it is tacitly assumed that the disk is wet so that the classical no-slip boundary condition can be applied at every point on the disk surface and the film flows under a planar interface for entire period of spinning. Another important class of problems, viz. spreading of a liquid

[a)]Author to whom correspondence should be addressed; electronic mail: prabir.daripa@math.tamu.edu

drop on a rotating disk in connection with the spin-coating, has been studied by Troian *et al.*,[13] Melo *et al.*,[14] Moriarty *et al.*,[15] and others. These studies were concerned with the motion of the contact line on the spinning disk and its stability. A recent study by Wilson *et al.*[16] of a spreading thin drop on a rotating disk shows that the profile of the spreading film becomes flat except near the contact line where capillary ridge forms that ultimately leads to instability.

Matsumoto *et al.*[17] and Kitamura[18] considered the nonplanar free surface and studied the unsteady problem. Matsumoto *et al.*[17] assumed a hemispherical liquid blob on the wetted surface of the disk and numerically studied the spreading of the blob on a rotating surface and the role of different forces on the development of thin film. The present study is parallel to that of Kitamura[18] as both of these studies concern the unsteady development of a thin film on a rotating disk for an initial nonplanar free surface. Kitamura[18] considered a hemispheroidal-shaped liquid blob placed on the center of the disk, studied the evolution of film thickness on the surface using an expansion for the film thickness in powers of r^2, and obtained the composite transient film thickness. Thus, Kitamura's solution is valid for small values of r, whereas our solution (see next) is valid at all values of r for thin films.

In this article, we consider the dynamics of a thin liquid film (with uniform/nonuniform initial thickness) on an annular spinning disk initially covered entirely with the liquid. The annular disk also models a dry circular area at the center with the rest of the disk covered by liquid. The chief justification for the use of this type of disk is that the liquid moves radially outward by the action of centrifugal force, and the flow eventually becomes uniform at a sufficient distance from the center of the disk. In order to minimize the wastage of the expensive coating liquid which is used up for the formation of the thin film at $r<a$, this type of spinning disk is generally used for spin coating. We obtain an asymptotic solution for the thickness of the thin film as a function of r and t using an expansion for the film thickness in powers of a small parameter ϵ and applying the method of matched asymptotic expansion. This solution for small values of ϵ is valid for all values of r and t and can be used to calculate the thickness of the film with good accuracy at any point on the disk. Other quantities of interest, such as the effects of amount of liquid initially deposited or the type of initial distribution on final film thickness, the velocity field, and the rate at which the fluid is depleted from the disk during thinning process, are calculated using this asymptotic solution. Effects of initial topography of the free surface, surface tension, Froude number, and Reynolds number are also addressed. We qualitatively and quantitatively predict various features of the thinning process which agree well with the existing numerical and experimental results.

II. THEORETICAL ANALYSIS

We consider an axisymmetric flow of a thin film of an incompressible viscous liquid on a planar annular disk which rotates about axis z passing through its center. It has an inner and outer radius of R_0 and R, respectively, and has Q_0 amount of liquid deposited on its surface. Our aim is to analytically study the evolution of initial film thickness: $h(r,t=0)=\hat{\delta}(r)$, $R_0<r<R$. The appropriate characteristic length scales along the radial (r) and the vertical direction (z) are R_0 and H_0, respectively, where H_0 is the maximum value of the initial film thickness and is much smaller than the inner radius R_0 which in turn is much smaller than the outer radius R of the annular disk.

During the spin-off stage, the centrifugal force and the viscous shear across the film are of comparable magnitude. At this stage, the balance of these forces define a characteristic time scale t_c given by

$$t_c=\nu/(\Omega H_0)^2, \tag{1}$$

where Ω and ν are the uniform angular velocity of the disk and the kinematic viscosity of the fluid, respectively. We introduce the following dimensionless variables as

$$\begin{aligned} &t'=t_c\tau,\quad r'=R_0 r,\quad z'=H_0 z,\quad h'=H_0 h,\quad \hat{\delta}=H_0\delta,\\ &u'=U_0 u,\quad v'=(U_0/\sqrt{\epsilon \mathrm{Re}})v,\\ &w'=\epsilon U_0 w,\quad \text{and } p'=(\nu R_0^2\rho/H_0^2 t_c)p, \end{aligned} \tag{2}$$

where the characteristic velocity scale U_0 is defined as (R_0/t_c) and the primed variables denote the relevant dimensional quantities and the dimensionless parameter $\epsilon=H_0/R_0$ is very small according to our previous assumptions.

The next step in our analysis, which we do not present here in any detail, and can be constructed easily, is to nondimensionalize the relevant governing equations of motion, the interfacial conditions at $z=h(r,\tau)$, the no-slip condition on the disk surface $z=0$, and the initial conditions. Essentially, these equations are similar to the ones in Reisfeld *et al.*[19] In the interfacial conditions, it is assumed that adjacent to the liquid film at the free surface is a gas or liquid vapor, and that the viscosity ratio μ_g/μ_l, where μ_l and μ_g are the viscosities of the liquid and gas phases, respectively, is much less than unity. Moreover, any motion of the gas phase is neglected. Further it is assumed that all physical properties viz. viscosity, surface tension, etc., are constant. Based on these assumptions and above scaling, we find that the relevant parameters that enter into the problem defined by the dimensionless equations and initial/boundary conditions are the Reynolds number $\mathrm{Re}=U_0H_0/\nu\ (\equiv R_0H_0^3\Omega^2/\nu^2)$, the Froude number $\mathrm{Fr}=\sqrt{(\Omega^4R_0^2H_0^3/g\nu^2)}$ in which g is the gravity, and the Weber number $\mathrm{We}=(\sigma_0/R_0H_0^2\Omega^2\rho)$ in which ρ is the density and σ_0 is the coefficient of surface tension at the free surface of the thin film.

In order to construct an asymptotic solution of the problem for $\epsilon\ll 1$, the dependent variables in the problem are expanded in powers of ϵ according to the following ansatz

$$F(r,z,\tau)\sim F_0(r,z,\tau)+\epsilon F_1(r,z,\tau)+O(\epsilon^2). \tag{3}$$

On substituting this for each dependent variable in the problem, and equating terms of like orders, we obtain several problems as usual, each to be solved at each order. (These equations at various orders are similar to the ones in Reisfeld et al.[19] On solving equations of the zeroth-order system, we find

$$u_0 = r\left(hz - \frac{z^2}{2}\right), \tag{4}$$

$$v_0 = r, \tag{5}$$

$$w_0 = \frac{1}{3}z^3 - hz^2 - \frac{1}{2} r\, z^2 h_r, \tag{6}$$

$$p_0 = 0. \tag{7}$$

Similarly, we obtain the following solutions of the first-order system of equations

$$\begin{aligned}
u_1 &= \left\{ -\overline{\mathrm{Fr}}\, h_r + \overline{\mathrm{We}}\left[h_{rrr} + \frac{h_{rr}}{r} - \frac{h_r}{r^2} \right] \right\} \left[hz - \frac{z^2}{2} \right] \\
&\quad + \mathrm{Re}\left[r h_\tau \left(\frac{z^3}{6} - \frac{h^2 z}{2} \right) + \frac{r^2 h h_r}{24} z^4 + \frac{2}{9} r h^3 z^3 \right. \\
&\quad \left. - \frac{3}{5} r h^5 z - \frac{r^2 h^4 h_r}{6} z + \frac{r z^6}{360} - \frac{r h z^5}{60} \right], \\
v_1 &= \mathrm{Re}\left[\frac{r h z^3}{3} - \frac{2}{3} r h^3 z - \frac{r}{12} z^4 \right], \\
w_1 &= \frac{1}{r}\left[\overline{\mathrm{We}} \left\{ r \left[\frac{1}{r}(r h_r)_r \right]_r \right\}_r - \overline{\mathrm{Fr}}\,(r h_r)_r \right] \left(\frac{z^3}{6} - \frac{h z^2}{2} \right) \\
&\quad + \left[\overline{\mathrm{Fr}}\, h_r - \overline{\mathrm{We}} \left[\frac{1}{r}(r\, h_r)_r \right]_r \right] \left(\frac{h_r z^2}{2} \right) \\
&\quad + \mathrm{Re}\left[\frac{h z^6}{180} - \frac{z^7}{1260} - \frac{h^3 z^4}{9} + \frac{3h^5}{5} z^2 + \frac{r h_r}{360} z^6 \right. \\
&\quad - \frac{r h h_r}{40} z^5 - \frac{r h^2 h_r}{6} z^4 + \frac{7}{4} r h^4 h_r z^2 - \frac{r^2 h_r^2}{120} z^5 \\
&\quad + \frac{r^2 h^3 h_r^2}{3} z^2 - \frac{r^2 h h_{rr}}{120} z^5 + \frac{r^2 h^4 h_{rr}}{12} z^2 + \frac{h^2 h_\tau}{2} z^2 \\
&\quad \left. - \frac{h_\tau}{12} z^4 - \frac{r h_{r\tau}}{24} z^4 + \frac{r h^2 h_{r\tau}}{4} z^2 + \frac{r h h_r h_\tau}{2} z^2 \right].
\end{aligned} \tag{8}$$

In the aforementioned, we have used the symbols $\overline{\mathrm{Fr}} = \mathrm{Re}\,\mathrm{Fr}^{-2}$ and $\overline{\mathrm{We}} = \epsilon^2 \mathrm{We}$. Using equations for u_1 and w_1 from Eq. (8) in the kinematic boundary condition, $h_\tau + u h_r = w$, for u and w respectively, the long time evolution equation for h, accurate up to $O(\epsilon)$, becomes

$$\begin{aligned}
h_\tau &+ \frac{1}{3r}\left(r^2 h^3 - \epsilon \left\{ r h^3 \left[\overline{\mathrm{Fr}}\, h_r - \mathrm{We}\left(\frac{1}{r}[r h_r]_r \right)_r \right] \right. \right. \\
&\quad \left. \left. + \frac{\mathrm{Re}}{4}\left(\frac{5}{2} r^2 h^4 h_\tau + \frac{9}{10} r^3 h^6 h_r + \frac{311}{105} r^2 h^7 \right) \right\} \right)_r \\
&\quad + O(\epsilon^2) = 0,
\end{aligned} \tag{9}$$

which exactly matches with the Eq. (35) of Reisfeld *et al.*[19] with $E=0$. The present analysis deviates from that of Kitamura[18] in which an expansion of the film profile $h(r,\tau)$ in powers of r^2 is used to study the evolution of film thickness. Thus, Kitamura's analysis is valid near the rotational axis (at $r=0$) only. To get an asymptotic solution for small values of ϵ which is valid for all values of r, we instead expand the film profile $h(r,\tau)$ in powers of ϵ

$$h(r,\tau) \sim h_0(r,\tau) + \epsilon h_1(r,\tau) + O(\epsilon^2). \tag{10}$$

Using Eq. (10) in Eq. (9) and collecting the coefficients of orders up to ϵ, we obtain at the lowest order the following governing equation

$$h_{0\tau} + r h_0^2 h_{0r} = -\frac{2}{3} h_0^3, \tag{11}$$

while at order ϵ, we have

$$\begin{aligned}
h_{1\tau} + r h_0^2 h_{1r} &= -2(h_0^2 + r h_0 h_{0r}) h_1 \\
&\quad + \frac{1}{3r}\left[r h_0^3 \left\{ \overline{\mathrm{Fr}}\, h_{0r} - \overline{\mathrm{We}} \left[\frac{1}{r}(r h_{0r})_r \right]_r \right\} \right. \\
&\quad \left. + \mathrm{Re}\left(\frac{34}{105} r^2 h_0^7 - \frac{2}{5} r^3 h_0^6 h_{0r} \right) \right]_r.
\end{aligned} \tag{12}$$

It follows from Eq. (11) that

$$\frac{d}{d\tau} h_0(r(\tau),\tau) = -\frac{2}{3} h_0^3(r(\tau),\tau), \tag{13}$$

along the characteristic curve $r(\tau)$ satisfying

$$\frac{d}{d\tau} r(\tau) = r(\tau) h_0^2(r(\tau),\tau). \tag{14}$$

Upon integration, Eqs. (13) and (14) give

$$\begin{aligned}
h_0(r(\tau),\tau) &= c_0 \left(1 + \frac{4}{3} c_0^2 \tau \right)^{-1/2} \\
\text{along } r(\tau) &= c_1 \left(1 + \frac{4}{3} c_0^2 \tau \right)^{3/4}.
\end{aligned} \tag{15}$$

It also follows from Eq. (15) that, along each characteristic curve [Eq. (14)],

$$r(\tau) h_0^{3/2}(r(\tau),\tau) = c_1 c_0^{3/2} = \text{constant}. \tag{16}$$

Here c_0 and c_1 are characteristic-curve-dependent constants. Since Eqs. (15) and (16) are valid at large times, these constants c_0 and c_1 can be related to initial data by matching these solutions with small time solutions which we discuss later in Sec. III. These two equations in Eq. (15) can be combined to obtain

$$r(\tau) = c_1 h_0^{-3/2}(r(\tau),\tau) \left(\frac{1}{h_0^2(r(\tau),\tau)} - \frac{4}{3}\tau \right)^{-3/4}, \tag{17}$$

which is in agreement with the works of Melo *et al.*[14] and Moriarty *et al.*[15] on the spreading of a drop on a rotating disk.

Similarly, it follows from Eq. (12) that h_1 can be integrated along the same characteristic curve [Eq. (14)]. In so doing, we obtain

$$h_1(r(\tau),\tau)=-\frac{2}{9}\overline{\mathrm{Fr}}\,c_0^2c_1^{-2}\chi^{-5/2}+\frac{32}{81}\overline{\mathrm{We}}\,c_0^2c_1^{-4}\chi^{-4}+\frac{62}{315}\mathrm{Re}\,c_0^5\chi^{-5/2}+c_2\chi^{-1/2}, \tag{18}$$

along the characteristic curve [Eq. (14)]. In Eq. (18), $\chi=(1+4c_0^2\tau/3)$ and c_2 is the constant of integration. In order to find the constants c_0, c_1, c_2 by matching these solutions with short time solutions, we next find short time solutions.

A. Short-time analysis

At the spun-up stage, the time scale is dictated by the fact that the local inertial term is of the same order of magnitude as the viscous and the centrifugal terms in the governing equations. The appropriate time scale is then given by

$$t=\tau/\epsilon,\quad \bar{u}=u,\quad \bar{v}=v,\quad \bar{w}=w,\quad \bar{h}=h,\quad \bar{p}=p,\quad \bar{r}=r,\quad \text{and}\quad \eta=z. \tag{19}$$

where notations are introduced for short-time solutions for all other variables. The governing equations of motion and associated boundary/initial conditions are then written in terms of these variables. As before, expanding the scaled dependent variables in powers of ϵ [see Eq. (3)] and substituting these in these scaled equations and associated boundary/initial conditions, we separate equations of like orders. This gives several problems, as usual, one at each order. On solving the problem at zeroth order, we find

$$\bar{h}_0(\bar{r},t)=\delta(\bar{r}),\quad \text{for } t\geqslant 0,\quad 1\leqslant\bar{r}<R/R_0. \tag{20}$$

$$\begin{aligned}\bar{u}_0(\bar{r},\alpha,t)=\bar{r}\Bigg[&\delta^2(\bar{r})\left(\alpha-\frac{\alpha^2}{2}\right)-2\,\delta^2(\bar{r})\sum_{p=1(2)}^{\infty}\frac{\sin(\lambda_p\alpha)}{\lambda_p^3}\exp(-\lambda_p^2t/\mathrm{Re}\,\delta^2(\bar{r}))\\&-\frac{4t}{\mathrm{Re}}\sum_{p=1(2)}^{\infty}\frac{(\sin\lambda_p\alpha)}{\lambda_p}\exp(-\lambda_p^2t/\mathrm{Re}\,\delta^2(\bar{r}))-16\sum_{p=1(2)}^{\infty}\sum_{n=1(2)}^{\infty}\frac{\delta^2(\bar{r})A_{np}^o}{(\lambda_p^2-2\lambda_n^2)}(\sin(\lambda_p\alpha)\,\{\exp(-\lambda_n^2t/\mathrm{Re}\,\delta^2(\bar{r}))\\&-\exp(-\lambda_p^2t/\mathrm{Re}\,\delta^2(\bar{r}))\})-32\sum_{p=1(2)}^{\infty}\sum_{n=1(2)}^{\infty}\sum_{\ell>n}^{\infty}\frac{\delta^2(\bar{r})A_{np}^{\ell}}{\lambda_p^2-(\lambda_n^2+\lambda_\ell^2)}\sin(\lambda_p\alpha)\\&\times\{\exp(-(\lambda_n^2+\lambda_\ell^2)t/\mathrm{Re}\,\delta^2(\bar{r}))-\exp(-\lambda_p^2t/\mathrm{Re}\,\delta^2(\bar{r}))\}\Bigg],\end{aligned}$$

$$\bar{v}_0(\bar{r},\alpha,t)=\bar{r}\left[1-2\sum_{n=1(2)}^{\infty}\frac{\sin(\lambda_n\alpha)}{\lambda_n}\exp(-\lambda_n^2t/\mathrm{Re}\,\delta^2(\bar{r}))\right], \tag{21}$$

$$\begin{aligned}\bar{w}_0(\alpha,t)=\;&\delta^3(\bar{r})\left(\frac{\alpha^3}{3}-\alpha^2\right)-4\,\delta^3(\bar{r})\sum_{p=1(2)}^{\infty}\frac{\cos(\lambda_p\alpha)-1}{\lambda_p^4}\exp(-\lambda_p^2t/\mathrm{Re}\,\delta^2(\bar{r}))-\frac{8t\,\delta(\bar{r})}{\mathrm{Re}}\sum_{p=1(2)}^{\infty}\frac{\cos(\lambda_p\alpha)-1}{\lambda_p^2}\\&\times\exp(-\lambda_p^2t/\mathrm{Re}\,\delta^2(\bar{r}))-32\delta^3(\bar{r})\sum_{p=1(2)}^{\infty}\sum_{n=1(2)}^{\infty}\frac{A_{np}^o}{\lambda_p(\lambda_p^2-2\lambda_n^2)}(\cos(\lambda_p\alpha)-1)\,\{\exp(-2\lambda_n^2t/\mathrm{Re}\,\delta^2(\bar{r}))\\&-\exp(-2\lambda_p^2t/\mathrm{Re}\,\delta^2(\bar{r}))\}-64\delta^3(\bar{r})\sum_{p=1(2)}^{\infty}\sum_{n=1(2)}^{\infty}\sum_{1>n}\frac{A_{np}^{\ell}\,\{\cos(\lambda_p\alpha)-1\}}{\lambda_p\,\{\lambda_p^2-\lambda_n^2-\lambda_\ell^2\}}(\{\exp[-(\lambda_n^2+\lambda_\ell^2)t/\mathrm{Re}\delta^2(\bar{r})]\\&-\exp[-\lambda_p^2t/\mathrm{Re}\,\delta^2(\bar{r})]\}),\end{aligned}$$

where $\eta=\alpha\delta(\bar{r})$, $\lambda_n=n\pi/2$, $n=1,3,5,\ldots$, $A_{np}^o=1/(\lambda_p(\lambda_p^2-4\lambda_n^2))$, and $A_{np}^{\ell}=\lambda_p/(\lambda_p^4+(\lambda_n^2-\lambda_\ell^2)^2-2\lambda_p^2(\lambda_n^2+\lambda_\ell^2))$. Since the free surface will vary within $0\leqslant\eta\leqslant\delta(\bar{r})\leqslant 1$ after the start of the rotation of the disk, we have assumed that $0\leqslant\alpha\leqslant 1$ in finding Eq. (20). To complete the solution, we need to calculate the first-order correction to the film thickness for short time. From the kinematic condition, we obtain the first-order correction to $\bar{h}_0(\bar{r},t)$ as

$$\overline{h_1}(\overline{r},t)=-\frac{2}{3}\delta^3(\overline{r})\,t-4\delta^5(\overline{r})\mathrm{Re}\sum_{p=1(2)}^{\infty}\left(\frac{\exp(-\lambda_p^2t/\mathrm{Re}\,\delta^2(\overline{r}))-1}{\lambda_p^6}\right)-\frac{8}{\mathrm{Re}}\sum_{p=1(2)}^{\infty}\frac{1}{\lambda_p^2}\left\{\frac{\mathrm{Re}\,\delta^3(\overline{r})t}{\lambda_p^2}\exp[-\lambda_p^2t/\mathrm{Re}\,\delta^2(\overline{r})]\right.$$
$$\left.+\frac{\mathrm{Re}^2\delta^5(\overline{r})}{\lambda_p^4}(\exp[-\lambda_p^2t/\mathrm{Re}\,\delta^2(\overline{r})]-1)\right\}-32\delta^5(\overline{r})\mathrm{Re}\sum_{p=1(2)}^{\infty}\sum_{n=1(2)}^{\infty}\frac{A_{np}^o}{\lambda_p(\lambda_p^2-2\lambda_n^2)}$$
$$\times\left\{\frac{\exp(-2\lambda_n^2t/\mathrm{Re}\,\delta^2(\overline{r}))-1}{2\lambda_n^2}-\frac{\exp(-\lambda_p^2t/\mathrm{Re}\,\delta^2(\overline{r}))-1}{\lambda_p^2}\right\}-64\delta^5(\overline{r})\mathrm{Re}\sum_{p=1(2)}^{\infty}\sum_{n=1(2)}^{\infty}\sum_{\ell>n}^{\infty}\frac{A_{np}^\ell}{\lambda_p\{\lambda_p^2-(\lambda_n^2+\lambda_\ell^2)\}}$$
$$\times\left\{\frac{\exp(-(\lambda_n^2+\lambda_\ell^2)t/\mathrm{Re}\,\delta^2(\overline{r}))-1}{(\lambda_n^2+\lambda_\ell^2)}-\frac{\exp(-\lambda_p^2t/\mathrm{Re}\,\delta^2(\overline{r}))-1}{\lambda_p^2}\right\}, \tag{22}$$

where $\overline{h_1}(\overline{r},0)=0$ is used. Comparing Eq. (22) with Eqs. (8a) and (8b) of Kitamura,[18] one can see that the terms for gravity and surface tension are absent from Eq. (22). This is due to the fact that the contributions of these terms in short-time analysis are of the order $O(\epsilon^2)$ and we have considered only up to $O(\epsilon)$. But the effects of these terms become prominent at large times [see Eqs. (8) and (12)].

B. Matched asymptotic solution

First we calculate c_0 and c_1 associated with Eq. (15) by using the matching condition that is derived from the requirement that the flow is continuous from spin-up to spin-off stage. This suggests

$$\lim_{t\to\infty}\overline{h_0}(t)=\lim_{\tau\to 0}h_0(\tau), \tag{23}$$

which implies

$$c_1=r(0)=\xi\,(\text{say}),\quad c_0=h_0(\xi,0)=\delta(\xi). \tag{24}$$

Therefore, to find $h_0(r,\tau)$, one solves the equation [second equation in Eq. (15)]

$$r(\tau)=\xi\left(1+\frac{4}{3}\tau\delta^2(\xi)\right)^{3/4}, \tag{25}$$

for ξ and then [first equation in Eq. (15)] uses

$$h_0(r,\tau)=\delta(\xi)\left(1+\frac{4}{3}\tau\delta^2(\xi)\right)^{-1/2}. \tag{26}$$

In order to find the first-order correction to the film thickness, we first need to find the constant c_2 that appears in Eq. (18). The constant c_2 in Eq. (18) can also be estimated through a matching relation [similar to relation (23)] between Eqs. (18) and (22), and this gives

$$-\frac{2}{9}\overline{\mathrm{Fr}}\,\delta^2(\xi)\xi^{-2}+\frac{32}{81}\overline{\mathrm{We}}\,\delta^2\xi^{-4}+\frac{62}{315}\mathrm{Re}\,\delta^5(\xi)+c_2$$
$$=0.660\,87\,\mathrm{Re}\,\delta^5(\xi). \tag{27}$$

Thus, we obtain $h_1(r,\tau)$ as

$$h_1(r,\tau)=\frac{32}{81}\overline{\mathrm{We}}\,\delta^2(\xi)\xi^{-4}\left(1+\frac{4}{3}\delta^2(\xi)\tau\right)^{-4}$$
$$+\left(\frac{62}{315}\mathrm{Re}\,\delta^5(\xi)-\frac{2}{9}\overline{\mathrm{Fr}\,\delta^2}(\xi)\xi^{-2}\right)$$
$$\times\left(1+\frac{4}{3}\delta^2(\xi)\tau\right)^{-5/2}+\left(\frac{2}{9}\overline{\mathrm{Fr}\,\delta^2}(\xi)\xi^{-2}\right.$$
$$\left.+0.463\,73\,\mathrm{Re}\,\delta^5(\xi)-\frac{32}{81}\overline{\mathrm{We}\,\delta^2}(\xi)\xi^{-4}\right)$$
$$\times\left(1+\frac{4}{3}\delta^2(\xi)\tau\right)^{-1/2}. \tag{28}$$

The composite uniform expansion (see Van Dyke)[20] for the transient film thickness $h^c(r,t)$ is then given by

$$h^c(r,\tau)=[h_0(r,\tau)+\overline{h_0}(r,\tau/\epsilon)-\delta(\xi)]+\frac{2}{3}\delta^3(\xi)\tau$$
$$+\epsilon[h_1(r,\tau)+\overline{h_1}(r,\tau/\epsilon)-0.660\,87\,\mathrm{Re}\,\delta^5(\xi)]. \tag{29}$$

III. RESULTS AND DISCUSSION

In any practical example of the spin coating process, one knows the inner radius R_0 of the annular disk, the maximum value H_0 of the initial film thickness, the coating fluid properties viscosity (μ), density (ρ), and surface tension (σ_0), and the rotational speed Ω of the disk. These dimensional values are then used to compute the parameters Re, We, and Fr (according to their definitions given in Sec. 2), the asymptotic parameter $\epsilon(=H_0/R_0)$, and the dimensionless film thickness by scaling the dimensional film thickness distribution with H_0. The calculation of the dimensionless composite film thickness h_c then proceeds from formula (29) which can then easily be interpreted in terms of dimensional numbers if necessary, as we show in the example next.

We show the evolution of the film thickness from two types of initial data: Nonuniform and almost uniform. First, we discuss our results for the following nonuniform initial distribution $h(r,0)=\delta(r)$, where

$$\delta(r)=1.089(r-1)^2e^{-(r-1)^{0.76}},\quad r\geqslant 1. \tag{30}$$

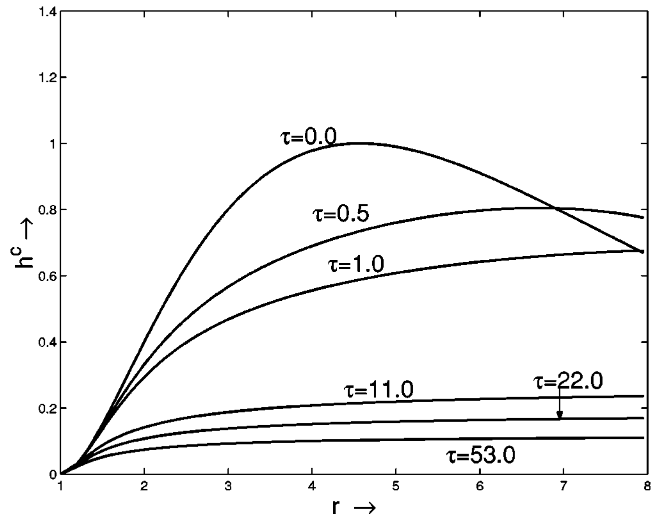

FIG. 1. Plots of the film thickness $h^c(r,\tau)$ vs r at several time levels with nonuniform initial distribution: $\delta(r)=1.089(r-1)^2e^{-(r-1)^{0.76}}$, $r\geqslant 1$.

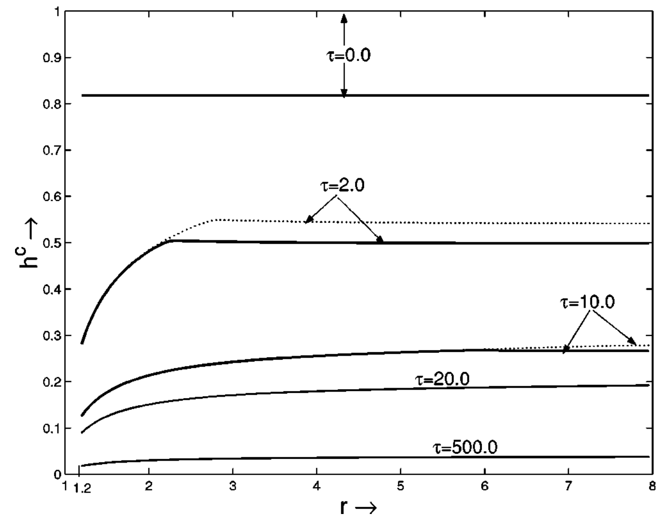

FIG. 2. Plots of the film height $h^c(r,\tau)$ vs r at several time levels with uniform initial distribution. Dotted and thin solid lines distinguish evolutions from two different initial data shown in plots for $\tau=0.0$.

These initial data were chosen from the consideration that the evolution of the film thickness be qualitatively consistent with the more realistic fluid profiles that one would observe in an industrial coating process. Figure 1 shows the initial film thickness $h^c(r,\,\tau)$ against r as well as some snapshots of its evolution at later times for Fr$=0.814\,382$, We $=6.839\,21$, Re $=0.721\,87$, and $\epsilon=0.1$. It is evident from Fig. 1 that the maximum height of the film quickly diminishes and the nonlinear profile becomes almost linear for $r>4$ or so at times $\tau>11$ (which is just over one second) approximately.

The aforementioned result can be interpreted in realistic terms: If we were to coat a typical compact disk (CD) size wafer with coating fluid (say) tricresyl phosphate, then we have $R_0=0.75$ cm, $H_0=0.075$ cm, $\mu=0.85$ g cm^{-1}s^{-1}, $\rho=1.16$ g cm^{-3}, and $\sigma_0=41.0$ dyn cm^{-1}. If the spinner is rotated with $\Omega=35$ rad per second (approximate 335 rpm) for 10 h, then the film reduces to a uniform film of thickness 1 μm (correct up to four decimal places) for $r>2.70$ cm (see Table I) from the center of the disk. In comparing this result with a regular CD, one finds that the coating is applied in the region 2.4 cm$\leqslant r \leqslant$6 cm approximately. The agreement is within acceptable limits considering that the calulation here is based on only a first-order asymptotic result. Other approximations are that the coating fluid is taken to be Newtonian and nonvolatile, and the end corrections are not incorporated, just to mention a few assumptions.

Next we discuss the effects of almost planar initial distributions on the final film thickness if two different amounts of liquid are initially deposited on the disk. We take the initial profile $h(r,0)=\delta_1(r)$ with

$$\delta_1(r)=C(1-\exp(100(1-r)),\quad r\geqslant 1, \tag{31}$$

where C is a suitable constant depending on different amounts of liquid. Figure 2 shows plots of the film height h^c against r at several time levels for two different choices of initial data of the form [Eq. (31)] with $C=1.0$ and C

TABLE I. Comparison of the film thickness $h^c(r,\tau)$ at several values of r in cm and time in h, when same amount of fluid Q_0 is distributed initially over a regular CD size wafer either as a nonuniform [Eq. (30)] or uniform [Eq. (31)] with $C=0.817\,732$ distribution.

	Time=0.0		Time=10 h	
Radial distance r (cm)	Uniform film distribution (cm)	Nonuniform film distribution (cm)	Uniform film distribution (cm)	Nonuniform film distribution (cm)
0.900	0.061 329 28	0.002 434 10	0.000 051 84	0.000 048 41
1.125	0.061 329 28	0.011 313 04	0.000 064 10	0.000 061 34
1.350	0.061 329 28	0.022 476 00	0.000 082 29	0.000 080 45
1.575	0.061 329 28	0.033 725 11	0.000 088 49	0.000 086 96
1.988	0.061 329 28	0.051 477 57	0.000 095 22	0.000 094 05
2.175	0.061 329 28	0.057 841 32	0.000 097 22	0.000 096 16
2.550	0.061 329 28	0.067 254 71	0.000 100 14	0.000 099 25
2.700	0.061 329 28	0.069 865 12	0.000 101 03	0.000 100 19
3.450	0.061 329 28	0.074 991 43	0.000 104 11	0.000 103 45
4.500	0.061 329 28	0.068 282 67	0.000 106 42	0.000 105 92
5.550	0.061 329 28	0.055 487 49	0.000 107 72	0.000 107 32
5.963	0.061 329 28	0.050 198 56	0.000 108 09	0.000 107 71

$=0.817\,732$. As the free surface evolves, the film remains almost planar with uniform thickness except for a very small region $r<2.55$ cm (details in Table I) around the inner ring where the fast transition from zero-film thickness to finite film thickness takes place. Figure 2 shows that the final film thickness does not depend on the amount of liquid initially deposited.

Next we compare the effects of the initial distributions: Nonuniform and almost planar on the final thickness if same amount of liquid is initially deposited. Table I presents the dimensional values of the film thickness for values of r in cm and time in h for two types of initial topography of the free surface: (i) Almost planar (with uniform) film thickness given by Eq. (31) with the constant $C=0.817\,732$; and (ii) nonplanar (for nonuniform) distribution of initial film thickness given by Eq. (30). In both cases, same amount of fluid Q_0 is deposited initially on the disk.

The free surface of the film in both cases become almost planar (except for a very small region around the inner ring) with uniform thickness at a later stage. For obvious reasons, the uniformity happens sooner when the film is initially uniform (see Table I). At this stage, the film for the case of nonuniform initial distribution is thinner as expected. However, the thinning process of the film continues beyond this stage and eventually, away from the inner ring, the film attains an almost uniform thickness that is independent of the initial distributions considered.

An explanation is given next as to why the film thins faster in the central region regardless of the type of distribution. Toward this end, we recall Eq. (28) which, after some manipulation with the help of Eqs. (17) and (24), becomes

$$h_1(r,\tau)=\frac{2}{9}\,\overline{\mathrm{Fr}}\,h_0^2 r^{-2}(\chi^2-1)+\frac{32}{81}\,\overline{\mathrm{We}}\,r^{-4}h_0^2(1-\chi^{7/2})$$
$$+\mathrm{Re}\;h_0^5\left(\frac{62}{315}+0.463\,73\chi^2\right), \tag{32}$$

where $\chi=(1+4\delta^2(\xi)\tau/3)$.

Now, one can see from Eq. 32 that the gravity (through Fr) and viscosity (through Re) do not help the thinning process of the film, and the effect of gravity is mild at $r\gg 1$. Equation (32) also shows that the term which represents the effect of surface tension (though $\overline{\mathrm{We}}$ is negative). This implies that surface tension helps in the thinning of the film. It is also clear from Eq. (32) that the effect of surface tension is more important near $r=1$ and negligible for larger r. As a result, surface tension helps in the thinning of the region around the inner ring more than in the thinning of the outer region. This thinning effect of the surface tension, as the free surface of the thin film evolves, is consistent with what physical forces impose on the present situation as explained next.

Since the entire surface of the disk is initially wet [see the initial data in Eqs. (30) and (31)] with finite film thickness, the radial outward flow which occurs everywhere as seen in Fig. 3 causes flattening of the free surface of the film that reduces the net free surface area of the film. Moreover, due to the gradual flattening of the free surface of the film, curvature effects are going to gradually impose less and less pressures on the fluid as the disk rotates. Energy released due to the reduction in the free surface area of the film and to the gradual reduction of curvature effects could be significant for a fluid with high surface tension. Thus, the physical effect that should happen is that a fluid with high surface tension should accelerate the radial outflow. This would increase the thinning rate as just noted. It is worth pointing out that the aforementioned result is contrary to that for the case of spreading of a drop, in which surface area increases with drop spreading due to the centrifugal force. Here, the surface tension resists the spreading of a drop for obvious reasons.

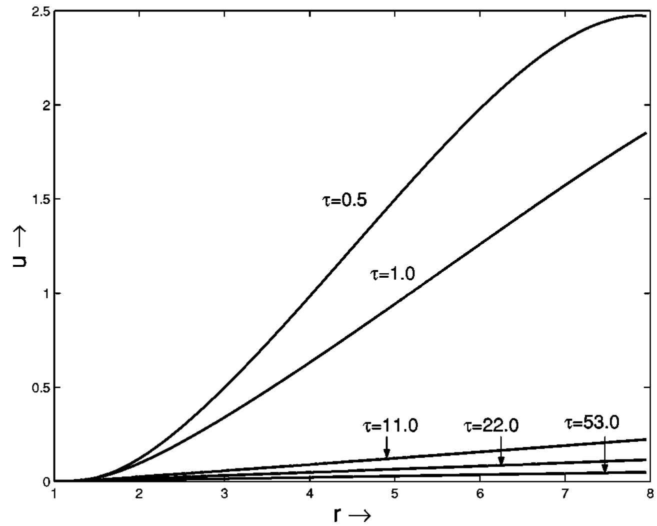

FIG. 3. Plots of free surface velocity component u vs r at several time levels for nonuniform initial distribution: $\delta(r)=1.089(r-1)^2 e^{-(r-1)^{0.76}}$, $r\geqslant 1$.

Figures 3–5, respectively, shows the plots of free surface velocity components u, v, and w against r at several values of time τ for the case of nonuniform initial data [Eq. (30)]. Figure 4 shows that the free surface azimuthal velocity com-

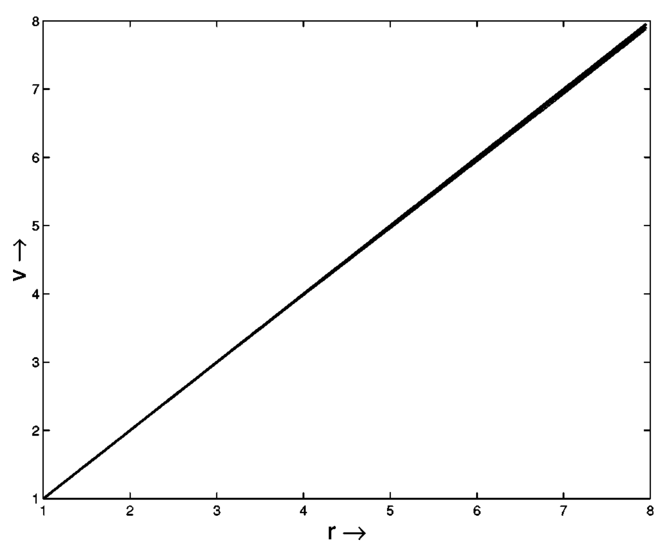

FIG. 4. Plots of free surface velocity component v vs r at same time levels as in Fig. 5 for nonuniform initial distribution: $\delta(r)=1.089(r-1)^2 e^{-(r-1)^{0.76}}$, $r\geqslant 1$. The variation in v is very small at different time levels and is linear with time. Hence, all of the plots fall within the very small region as shown.

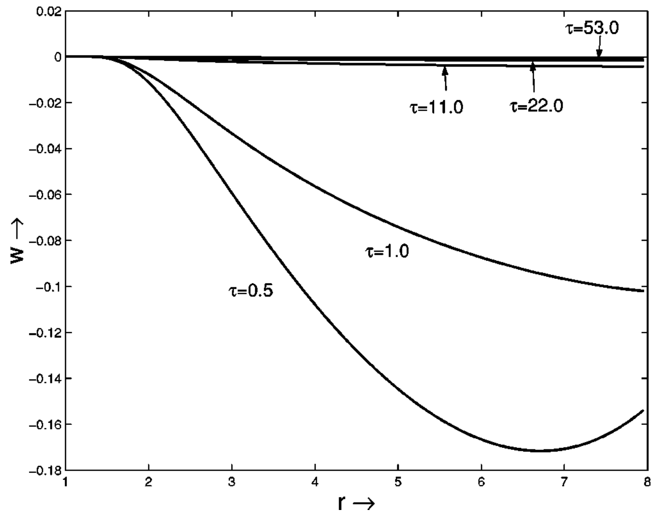

FIG. 5. Plots of free surface velocity component w vs r at several time levels for nonuniform initial distribution: $\delta(r)=1.089(r-1)^2e^{-(r-1)^{0.76}}$, $r \geqslant 1$.

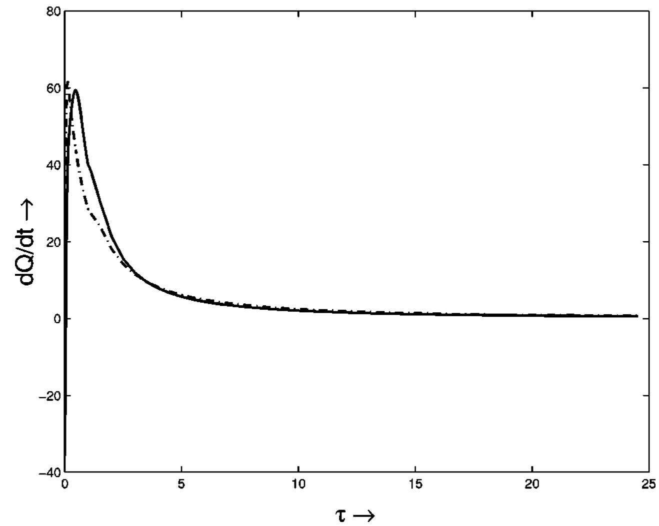

FIG. 6. Plots of the depletion rate $dQ/d\tau$ vs τ for uniform (–·– line) and nonuniform (thick dashed line) initial distributions, both corresponding to the same initial amount of liquid deposited initially. The nonuniform initial distribution: $\delta(r)=1.089(r-1)^2e^{-(r-1)^{0.76}}$, $r \geqslant 1$.

ponent, v, varies linearly with the radius just as it does on the surface of the rotating disk due to a no-slip condition. This is due to the fact that variation of v in the direction normal to the disk within the thin film is negligible. Figure 5 shows that the velocity component, w, normal to the disk is negligibly small. Figures 3 and 4 show that the radially outward velocity component, u, is the only significant velocity component (relative to the rotating disk).

The depletion rate, $dQ/d\tau$, is shown in Fig. 6 against time for both the nonuniform [Eq. (30)] and the uniform [Eq. (31)] initial data. Here, Q is the amount of liquid depleted in time τ and the initial amount of fluid Q_0 is the same in both cases. We find that most of the liquid flows out of the disk initially in a very short time in both cases. In particular, this Fig. 6 shows that the rate of depletion, at early stages of the development, is more for the uniform initial distribution than for the nonuniform one. In other words, the retention of fluid for nonuniform initial distribution is more than that for uniform distribution at early stages of the development of the thin film. At a later stage, the depletion rate decreases monotonically with increasing time and attains the same approximate value around $\tau=25$ (which in real time is less than but close to 3 s) for both initial distributions. This result is consistent with the fact that around time $\tau=25$, the nonuniform profile becomes almost flat away from the inner ring (see Fig. 1) and the uniform film thickness around $\tau=25$ depends very weakly on the initial uniform height of the film on the disk (see Fig. 2). The thinning rate eventually becomes zero at a very large time which is not shown in this figure.

IV. CONCLUSION

The asymptotic solution presented here sheds some light on the various phenomena associated with the film thinning process during spin coating. Some of these results explain experimentally observed facts and some provides insights into the spin-coating process.

We find that the final thickness of the almost planar thin film of uniform thickness does not depend on the initial topography (planar or nonplanar) of the free surface and on the initial amount of liquid deposited on the spinning disk. For the same amount of liquid deposited initially, the nonplanar initial free surface enhances film thinning when compared with the planar free surface. The surface tension is found to enhance film thinning near the central region during the thinning process. This conclusion is based on the $O(\epsilon)$ accurate asymptotic solution.

[1] P. L. Kapitza, Zh. Eksp. Teor. Fiz. **18**, (1948).
[2] A. C. Emslie, F. D. Bonner, and L. G. Peck, J. Appl. Phys. **29**, 858 (1958).
[3] R. G. Larson and T. G. Rehg, in *Liquid Film Coating*, edited by S. K. Kistler and P. M. Schweizer (Chapman and Hall, London, 1997), pp. 709–734.
[4] D. Meyerhofer, J. Appl. Phys. **49**, 3993 (1978).
[5] P. C. Sukanek, J. Imaging Technol. **11**, 184 (1985).
[6] S. A. Jenekhe and S. A. Schuldt, Ind. Eng. Chem. Fundam. **23**, 432 (1984).
[7] C. J. Lawrence, Phys. Fluids **31**, 2786 (1988).
[8] B. G. Higgins, Phys. Fluids **29**, 3522 (1986).
[9] B. S. Dandapat and P. C. Ray, Int. J. Non-Linear Mech. **25**, 569 (1990).
[10] B. S. Dandapat and P. C. Ray, J. Phys. D **27**, 2041 (1994).
[11] B. S. Dandapat and P. C. Ray, Z. Angew. Math. Mech. **78**, 635 (1998).
[12] P. C. Ray and B. S. Dandapat, J. Mech. Appl. Math. **47**, 297 (1992).
[13] S. M. Troian, E. Herbolzheimer, S. A. Safran, and J. F. Joanny, Europhys. Lett. **63**, 25 (1989).
[14] F. Melo, J. F. Joanny, and S. Fauve, Phys. Rev. Lett. **63**, 1958 (1989).
[15] J. A. Moriarty, L. W. Schwartz, and E. O. Tuck, Phys. Fluids **3**, 733 (1991).
[16] S. K. Wilson, J. Fluid Mech. **413**, 65 (2001).
[17] Y. Matsumoto, T. Ohara, T. Teruya, and H. Ohashi, JSME Int. J., Ser. II **32**, 52 (1989).
[18] A. Kitamura, Phys. Fluids **12**, 2141 (2000).
[19] B. Reisfeld, S. G. Bankoff, and S. H. Davis, J. Appl. Phys. **70**, 5258 (1991).
[20] M. Van Dyke, *Perturbation Methods in Fluid Mechanics* (Academic, New York, 1964).